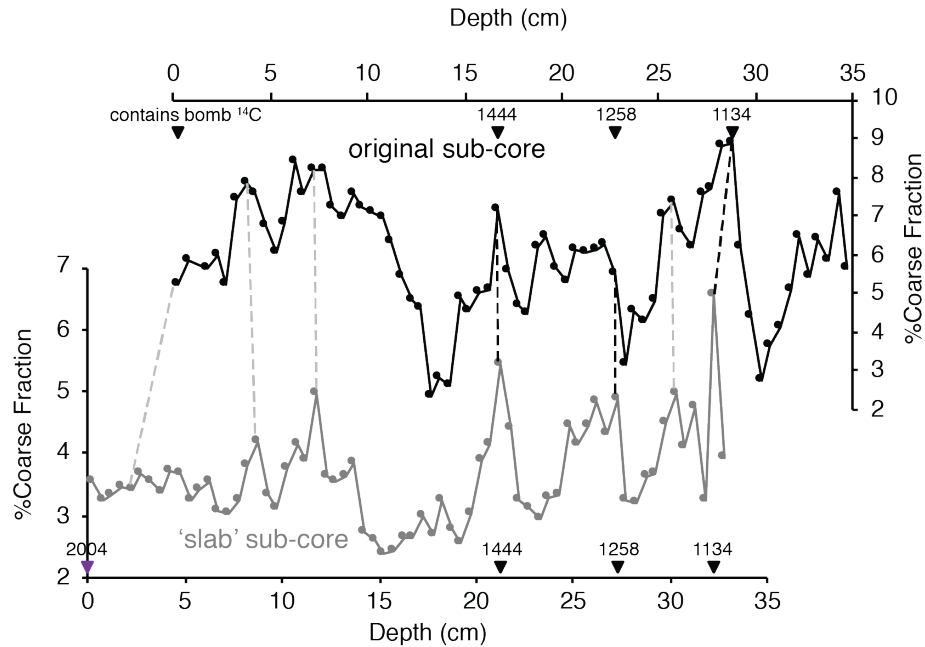
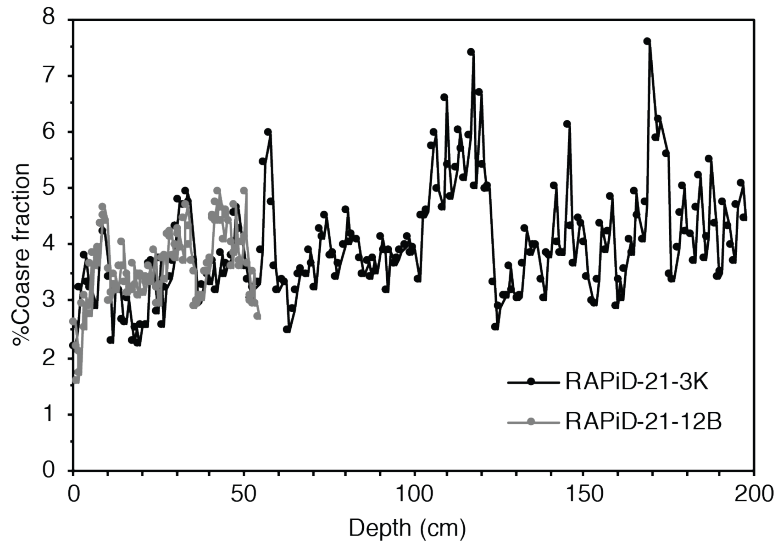


Supplementary Material

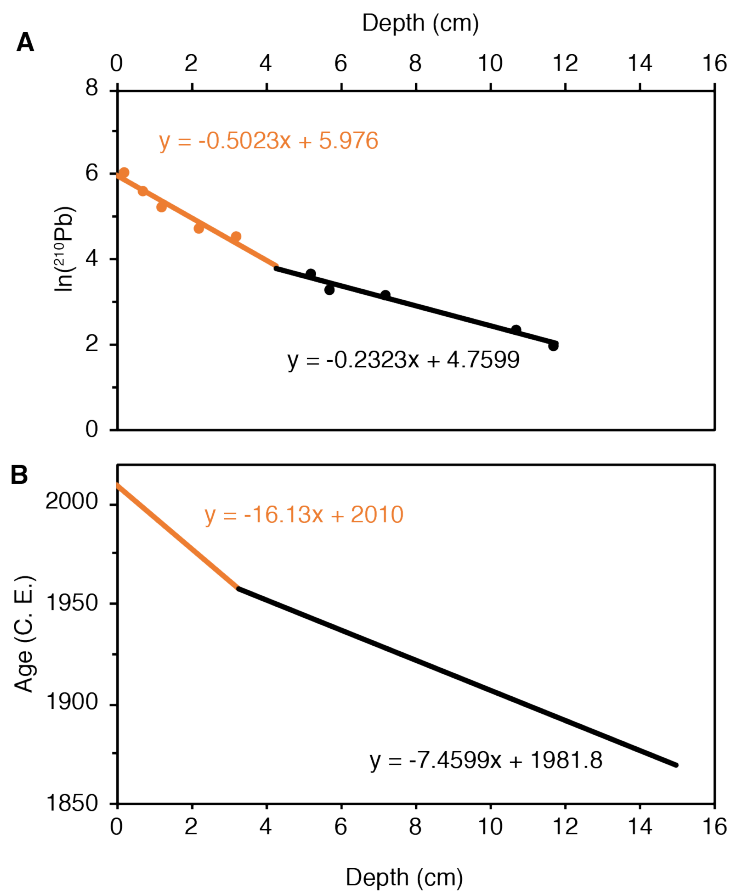
1 Supplementary Figures



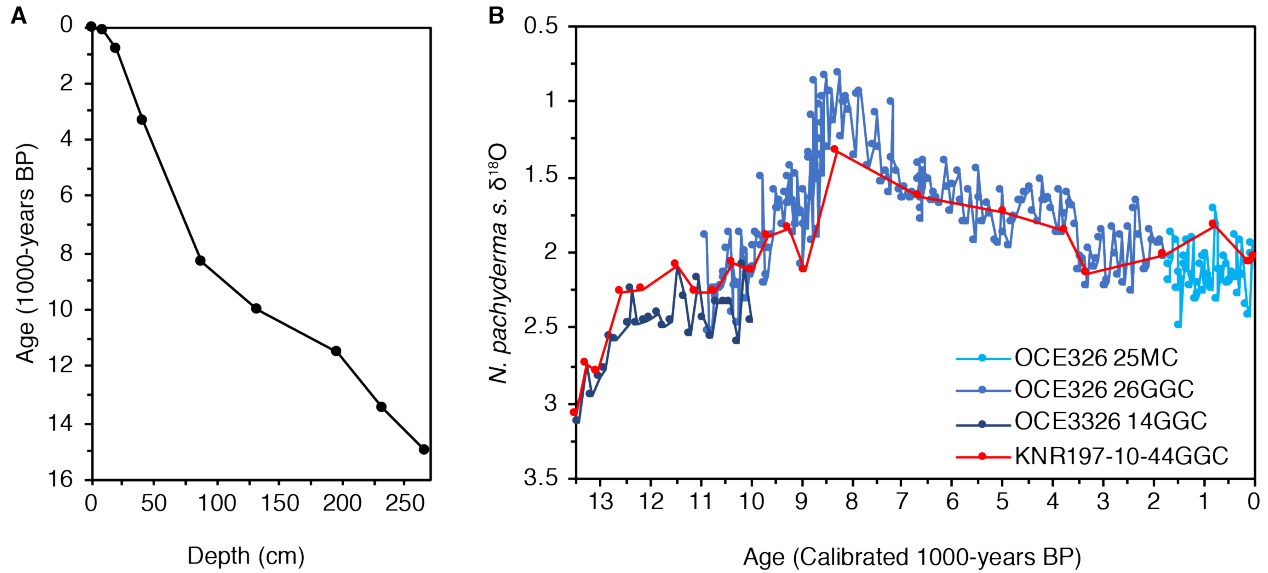
Supplementary Figure 1. Age-depth tie-points for RAPiD-35-25B. Alignment of the ‘slab’ sub-core (this study) to the original sub-core (Moffa-Sánchez et al., 2014), black dashed lines, is based on common features in their percent coarse fraction records. Grey dashed lines indicate additional comparable features seen in both records. Age constraints are provided from the original sub-core (Moffa-Sánchez et al., 2014). The core-top of the ‘slab’ sub-core is assumed have a modern age, 2004 (purple triangle).



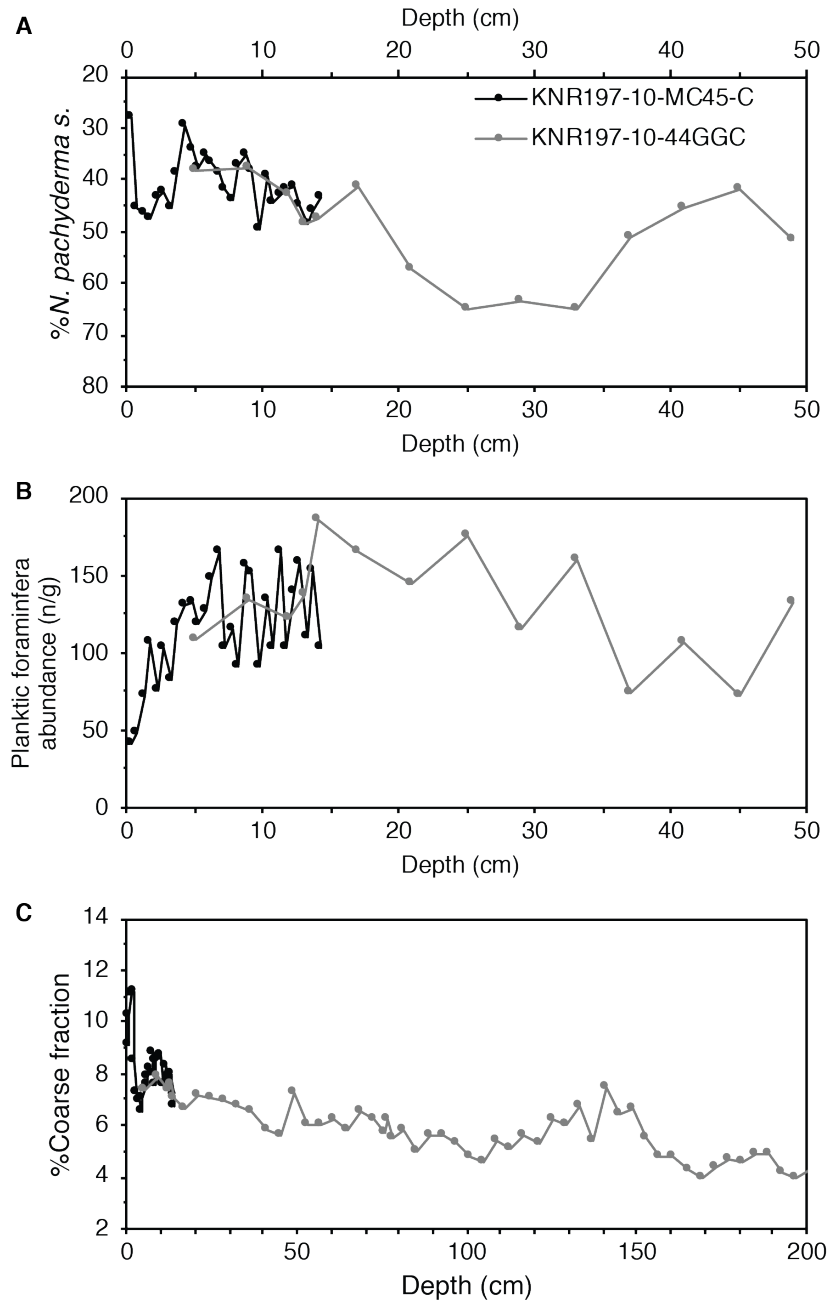
Supplementary Figure 2. Comparison of percent coarse fraction in cores RAPiD-21-12B and RAPiD-21-3K (Moffa-Sánchez and Hall, 2017).



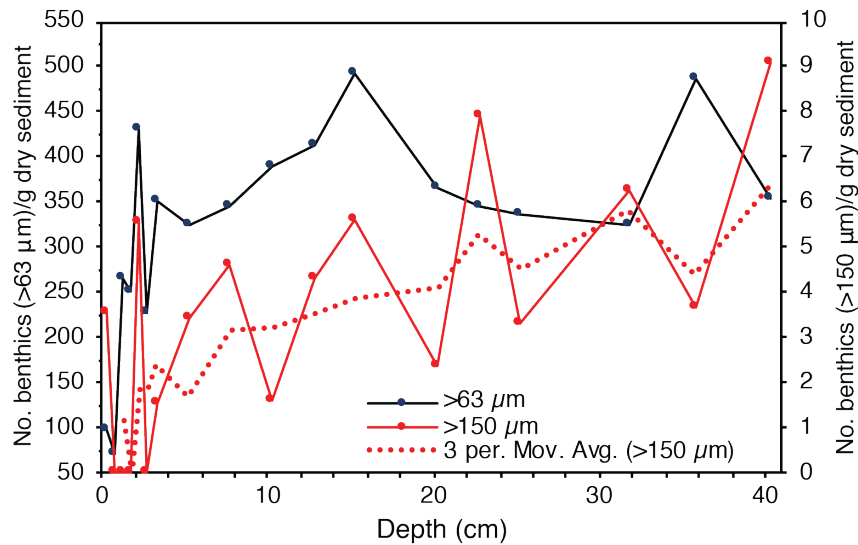
Supplementary Figure 3. Age model for KNR197-10-MC45-C. (A) Excess ^{210}Pb activity versus depth, sedimentation rate is estimated from the slope of the regression. (B) Age versus depth, ages were calculated from sedimentation rates.



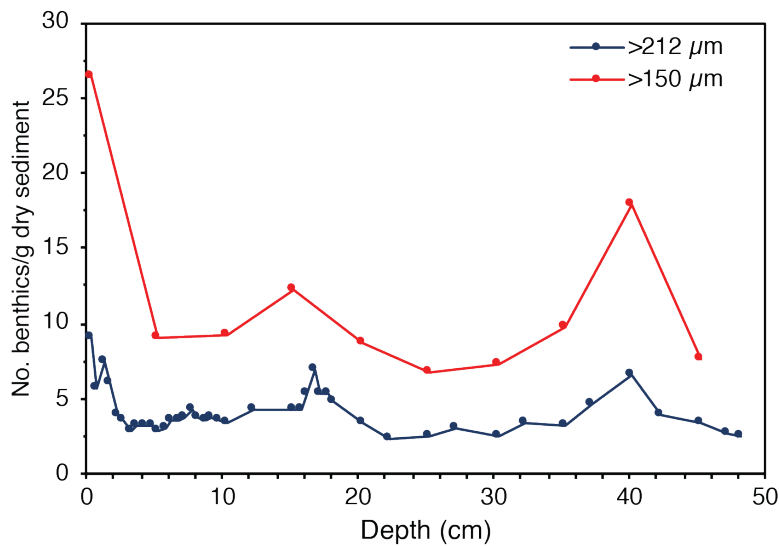
Supplementary Figure 4. (A) Age model for KNR197-10-44GGC. Age-depth tie points are based on $\delta^{18}\text{O}$ measurements measured on *N. pachyderma* and ^{210}Pb data measured on bulk sediment. *N. pachyderma s.* $\delta^{18}\text{O}$ measurements were tuned to *N. pachyderma s.* $\delta^{18}\text{O}$ data from Laurentian Fan sites. (B) *N. pachyderma s.* $\delta^{18}\text{O}$ data from KNR197-10-44GGC tuned to *N. pachyderma s.* $\delta^{18}\text{O}$ data from OCE3326 14GGC, OCE326 26GGC and OCE326 25MC (Laurentian Fan sediments; Keigwin et al., 2005).



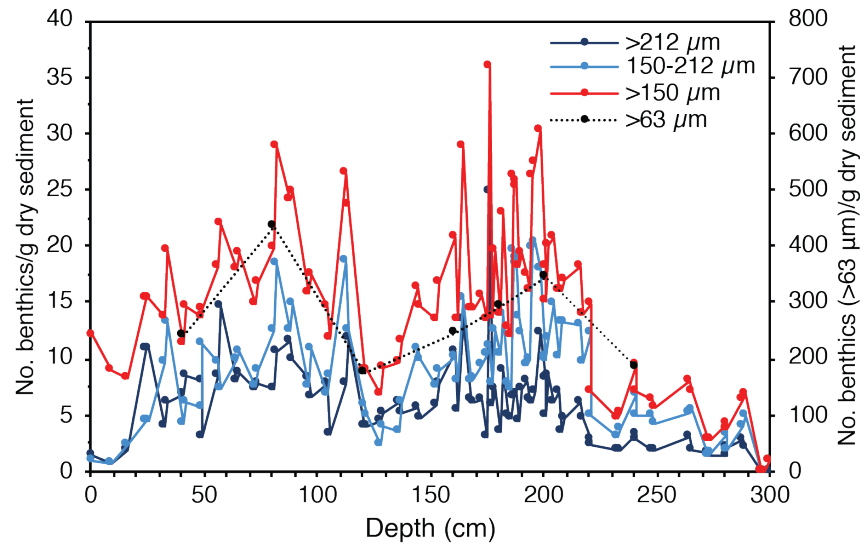
Supplementary Figure 5. Overlap of planktic foraminifera species counts and % coarse fraction data in KNR197-10-44GGC and KNR197-10-MC45-C. (A) Percent *N. pachyderma* s.. (B) Planktic foraminifera abundance. (C) Percent coarse fraction. Depths for KNR197-10-44GGC are adjusted by +4.5 cm to bring the cores into alignment. Percent coarse fraction values for KNR197-10-MC45-C are adjusted by -1.5 %.



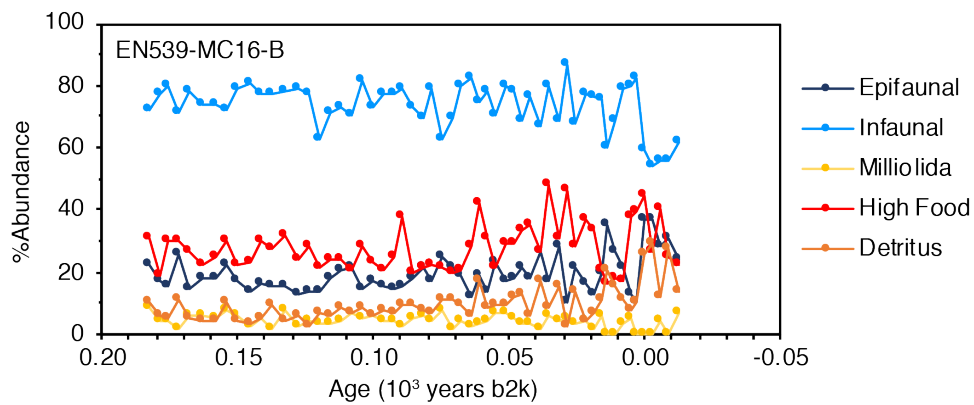
Supplementary Figure 6. Benthic abundances (n/g) in RAPiD-21-3K (Reyk R) in the >63 μm and >150 μm size fractions. 3-point moving average shown for >150 μm fraction because >150 μm count numbers are very low and therefore noisy.



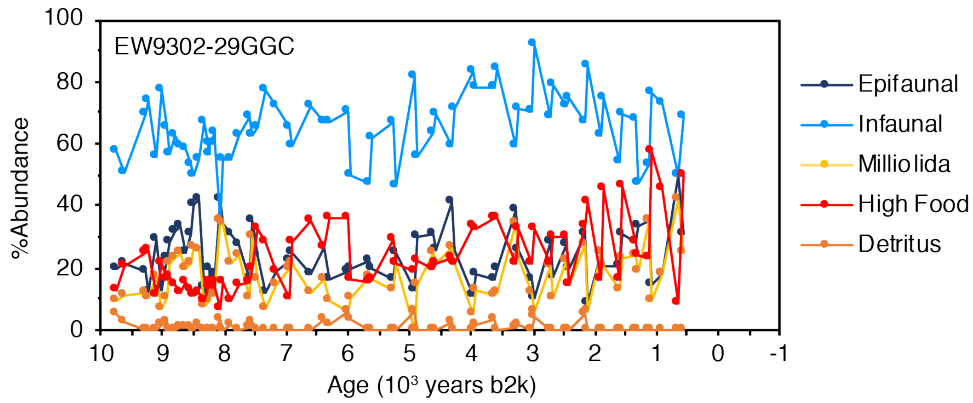
Supplementary Figure 7. Benthic abundances (n/g) in EN539-MC25-A in the >150 μm and >212 μm size fractions.



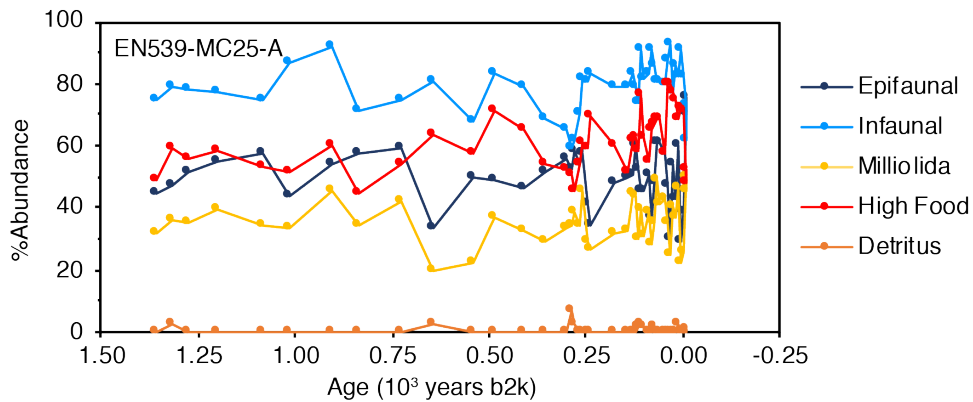
Supplementary Figure 8. Benthic abundances (n/g) in EW9302-29GGC in the >63 μm , >150 μm , 150-212 μm and >212 μm size fractions.



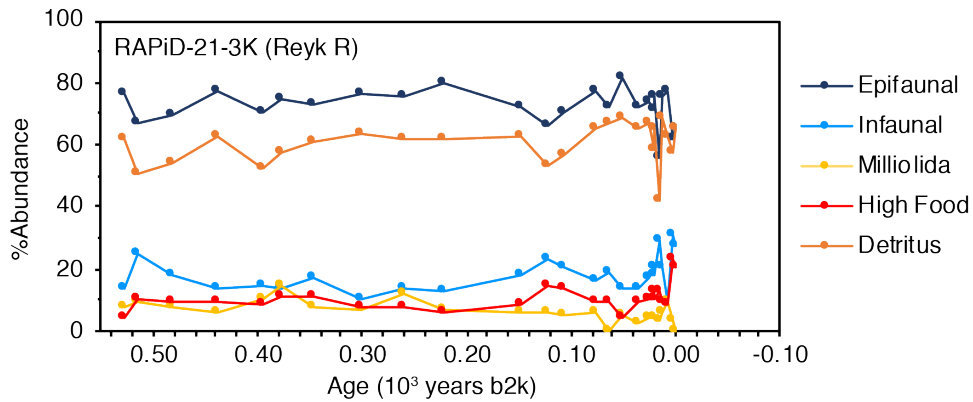
Supplementary Figure 9. %Abundances of different benthic groups in EN539-MC16-B. Benthic species are categorized by habitat (epifaunal/infaunal) and feeding characteristics (detritus - phytodetritus feeders, *Miliolida*, high food - high food depending foraminifera (Smart et al., 2019)). %Abundance totals do not sum 100% since some species were not defined by these categories (e.g., where there was uncertainty in the literature as to whether a species was epifaunal or infaunal), while other species are included in more than one category.



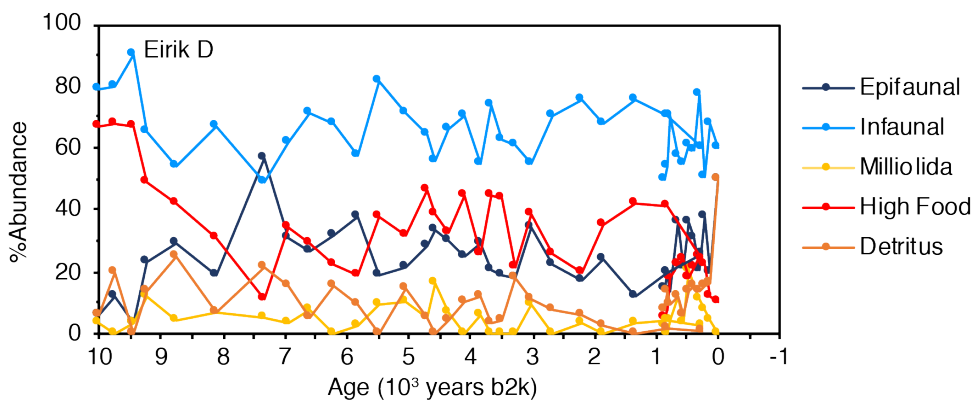
Supplementary Figure 10. %Abundances of different benthic groups in EW9302-29GGC. Benthic species are categorized by habitat (epifaunal/infaunal) and feeding characteristics (detritus - phytodetritus feeders, *Miliolida*, high food - high food depending foraminifera (Smart et al., 2019)). %Abundance totals do not sum 100% since some species were not defined by these categories (e.g., where there was uncertainty in the literature as to whether a species was epifaunal or infaunal), while other species are included in more than one category.



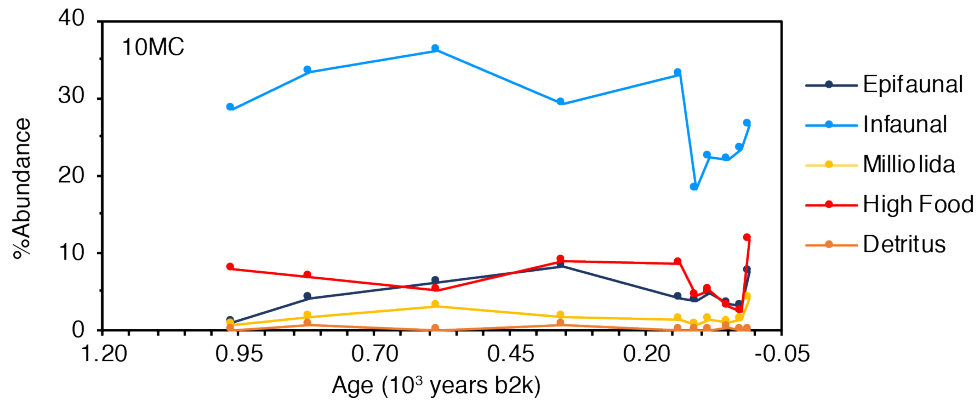
Supplementary Figure 11. %Abundances of different benthic groups in EN539-MC25-A. Benthic species are categorized by habitat (epifaunal/infaunal) and feeding characteristics (detritus - phytodetritus feeders, *Miliolida*, high food - high food depending foraminifera (Smart et al., 2019)). %Abundance totals do not sum 100% since some species were not defined by these categories (e.g., where there was uncertainty in the literature as to whether a species was epifaunal or infaunal), while other species are included in more than one category.



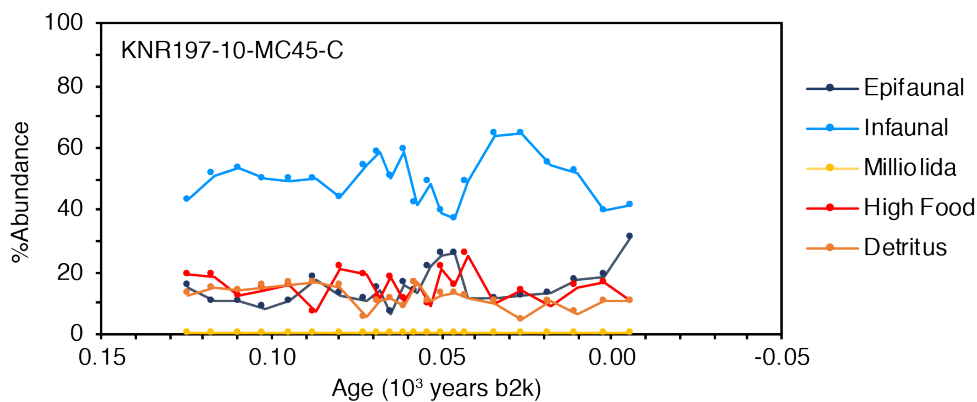
Supplementary Figure 12. %Abundances of different benthic groups in RAPID-21-3K (Reyk R). Benthic species are categorized by habitat (epifaunal/infaunal) and feeding characteristics (detritus - phytodetritus feeders, *Miliolida*, high food - high food depending foraminifera (Smart et al., 2019)). %Abundance totals do not sum 100% since some species were not defined by these categories (e.g., where there was uncertainty in the literature as to whether a species was epifaunal or infaunal), while other species are included in more than one category.



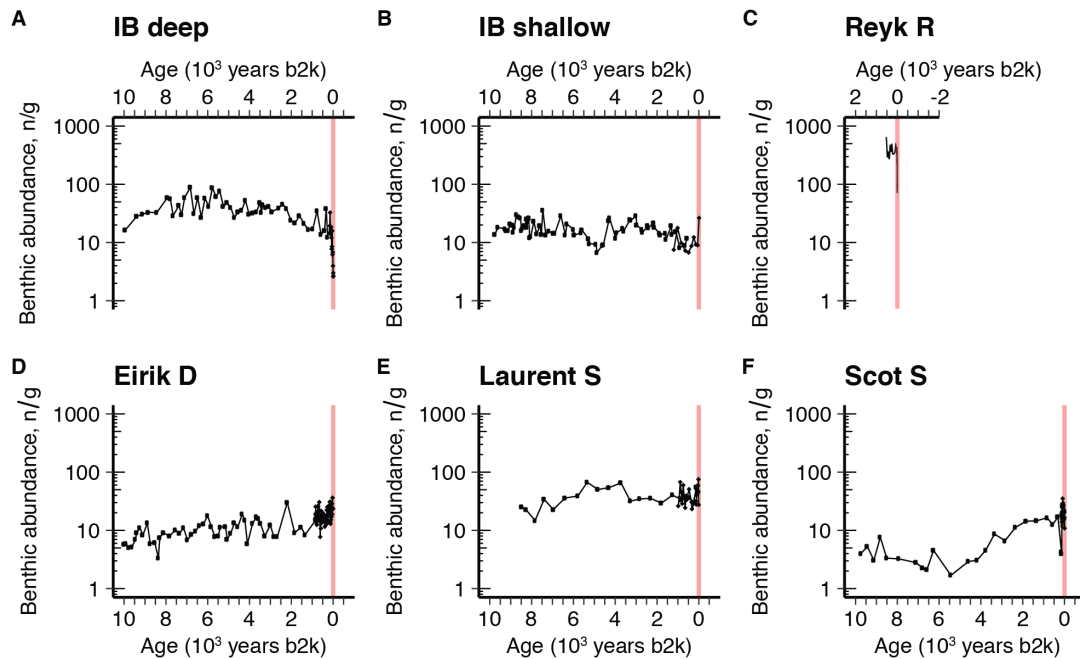
Supplementary Figure 13. %Abundances of different benthic groups in Eirik D. Benthic species are categorized by habitat (epifaunal/infaunal) and feeding characteristics (detritus - phytodetritus feeders, *Miliolida*, high food - high food depending foraminifera (Smart et al., 2019)). %Abundance totals do not sum 100% since some species were not defined by these categories (e.g., where there was uncertainty in the literature as to whether a species was epifaunal or infaunal), while other species are included in more than one category.



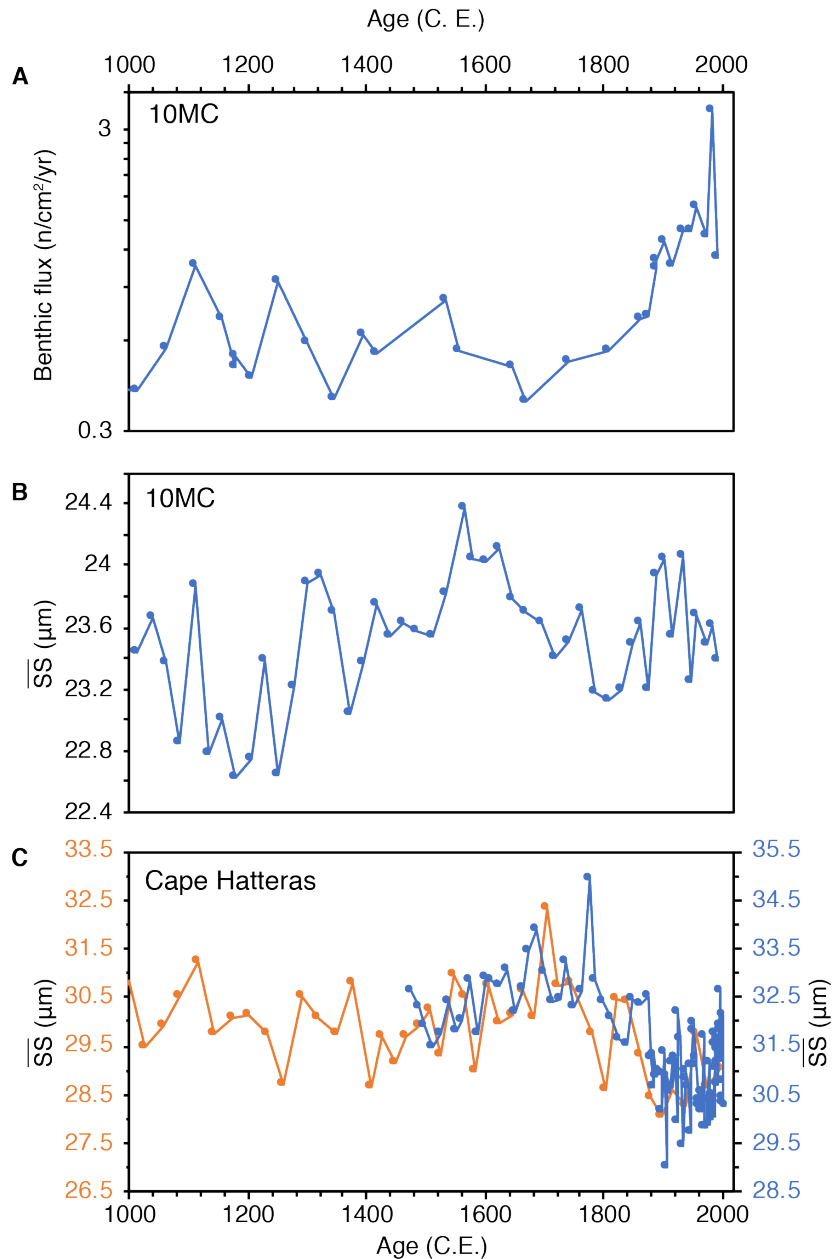
Supplementary Figure 14. %Abundances of different benthic groups in KNR158-4-10MC. Benthic species are categorized by habitat (epifaunal/infaunal) and feeding characteristics (detritus - phytodetritus feeders, *Miliolida*, high food - high food depending foraminifera (Smart et al., 2019)). %Abundance totals do not sum 100% since some species were not defined by these categories (e.g., where there was uncertainty in the literature as to whether a species was epifaunal or infaunal), while other species are included in more than one category.



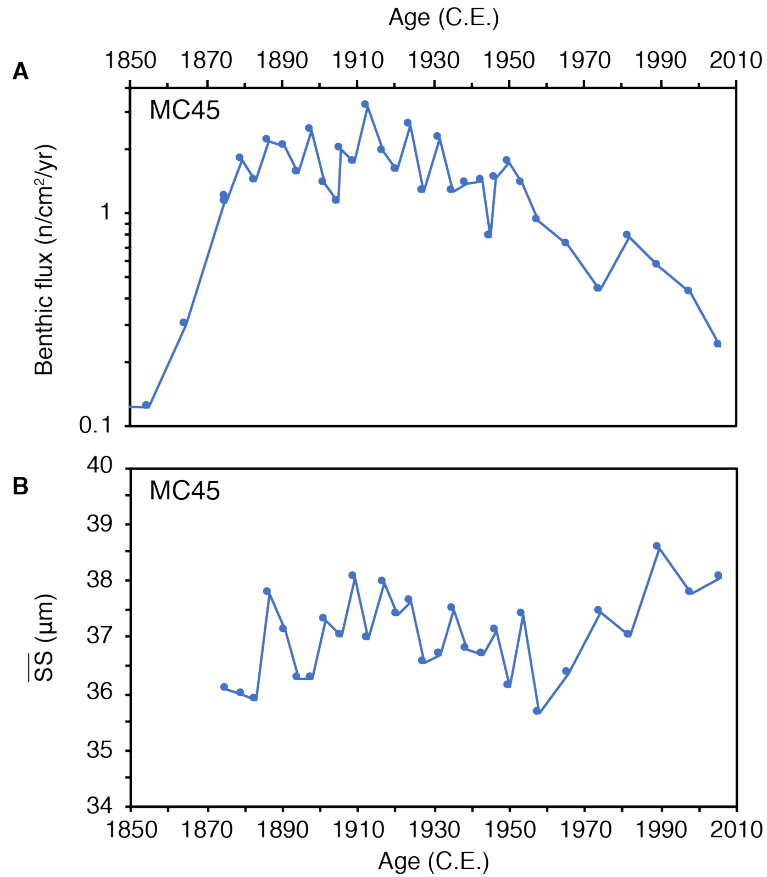
Supplementary Figure 15. %Abundances of different benthic groups in KNR197-10-MC45-C. Benthic species are categorized by habitat (epifaunal/infaunal) and feeding characteristics (detritus - phytodetritus feeders, *Miliolida*, high food - high food depending foraminifera (Smart et al., 2019)). %Abundance totals do not sum 100% since some species were not defined by these categories (e.g., where there was uncertainty in the literature as to whether a species was epifaunal or infaunal), while other species are included in more than one category.



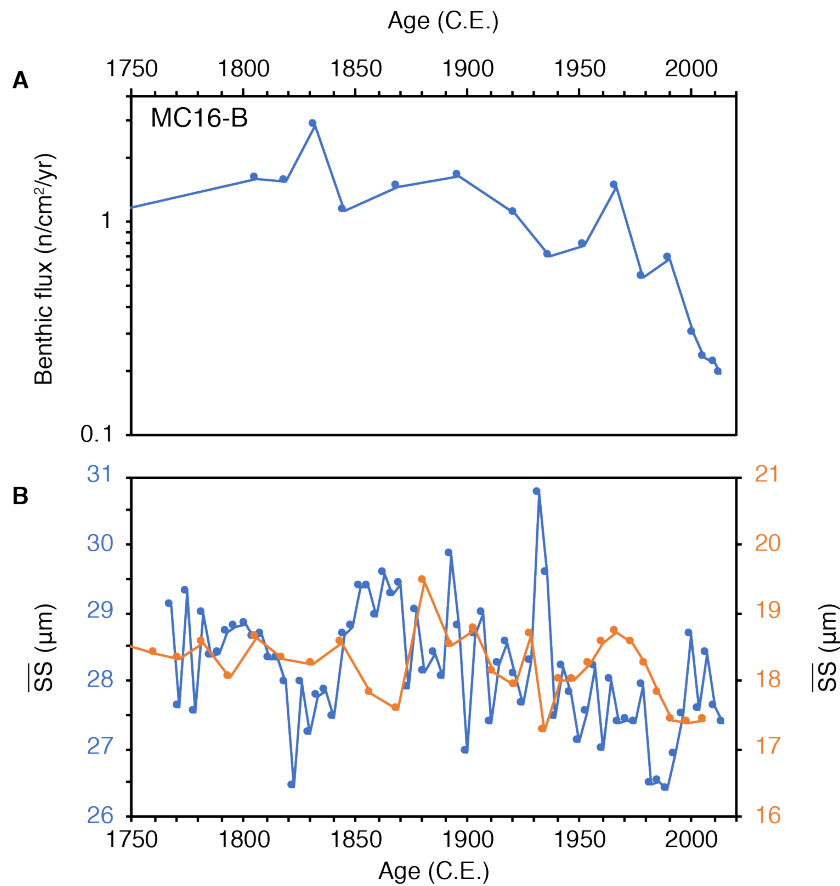
Supplementary Figure 16. Benthic abundance, n/g, in (A, B, C) Northeast Atlantic; (D) Labrador Sea; (E) Laurentian slope; and, (F) Scotian slope cores. Vertical red-shaded bars highlight the industrial era. Trends in benthic abundance, n/g, show very similar patterns to benthic fluxes, $\text{n/cm}^2/\text{yr}$ (Figs. 3, 4, 5) suggesting that trends in benthic fluxes are not an age model-artifact.



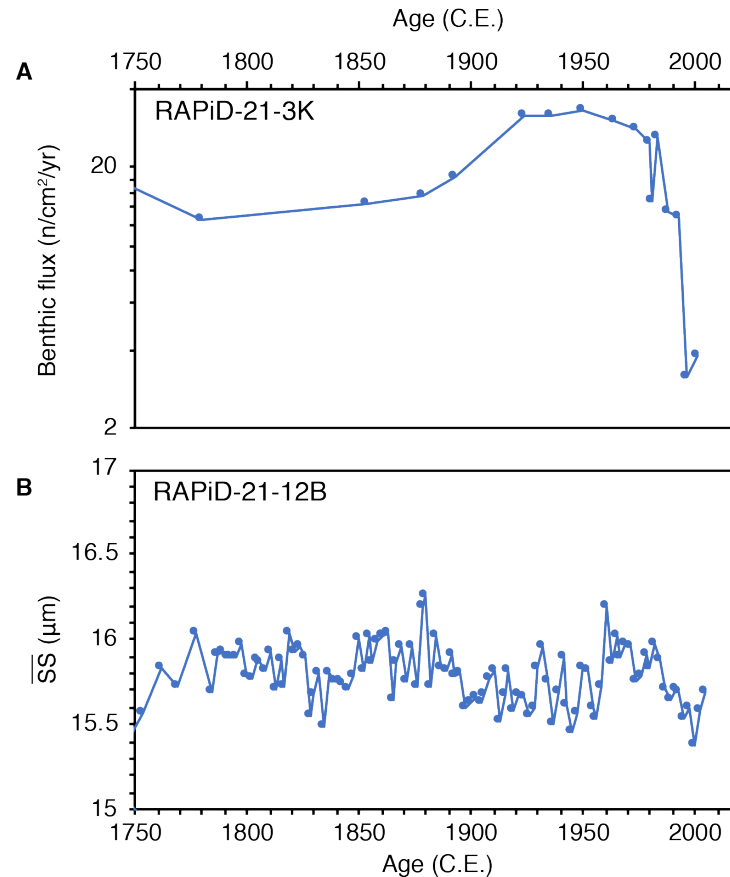
Supplementary Figure 17. Benthic flux and sortable silt records from the Northwest Atlantic. (A) KNR158-4-10MC benthic flux; (B) KNR158-4-10MC sortable silt mean grain size (unpublished data generated using the same procedures as described in Thornalley et al., 2018); (C) sortable silt mean grain size records from further south at Cape Hatteras (Thornalley et al., 2018). Mean sortable silt grain size is presented as a proxy for the vigor of near-bottom currents. If lateral advection of food supply is a strong control on benthic accumulation rates a positive correlation (high accumulation rates associated with increased bottom current strength) would be expected; inconsistent relationships between benthic fluxes and sortable size mean grain size suggest this is not the case, as shown here. At Cape Hatteras, sortable silt records an industrial era decrease in flow at 1.7 km (blue data) and 2 km (orange data) water depth.



Supplementary Figure 18. Benthic flux and sortable silt records showing differing trends from KNR197-10-MC45-C, Scotian slope, Northwest Atlantic. (A) benthic flux; (B) sortable silt mean grain size (this study).



Supplementary Figure 19. Benthic flux and sortable silt records from the Iceland Basin, Northeast Atlantic. (A) EN539-MC16-B benthic flux; (B) sortable silt mean grain size data from EN539-MC16-A (blue; unpublished data) and the nearby northern Gardar Drift (orange; Mjell et al., 2016). Sortable silt values suggest a slight decrease in the vigor of near-bottom water currents over the past few decades, but this change is minor compared to the decrease in benthic fluxes; and is therefore unlikely the key control on the decline in benthic fluxes given accompanied large changes in %*T. quinqueloba* and %*O. universa*.



Supplementary Figure 20. Benthic flux and sortable silt records from RAPiD-21-3K/12B, Northeast Atlantic. (A) benthic flux; (B) sortable silt mean grain size (Boessenkool et al., 2007).

References

- Boessenkool, K.P., Hall, I.R., Elderfield, H., and Yashayaev, I. (2007). North Atlantic climate and deep-ocean flow speed changes during the last 230 years. *Geophys. Res. Lett.* 34(13). doi: 10.1029/2007GL030285.
- Keigwin, L.D., Sachs, J.P., Rosenthal, Y., and Boyle, E.A. (2005). The 8200 year B.P. event in the slope water system, western subpolar North Atlantic. *Paleoceanography* 20(2). doi: 10.1029/2004PA001074.
- Mjell, T.L., Ninnemann, U.S., Kleiven, H.F., and Hall, I.R. (2016). Multidecadal changes in Iceland Scotland Overflow Water vigor over the last 600 years and its relationship to climate. *Geophys. Res. Lett.* 43(5), 2111–2117. doi: 10.1002/2016GL068227.
- Moffa-Sánchez, P., and Hall, I.R. (2017). North Atlantic variability and its links to European climate over the last 3000 years. *Nat. Commun.* 8(1), 1726. doi: 10.1038/s41467-017-01884-8.

- Moffa-Sánchez, P., Hall, I.R., Barker, S., Thornalley, D.J., and Yashayaev, I. (2014). Surface changes in the eastern Labrador Sea around the onset of the Little Ice Age. *Paleoceanography* 29(3), 160–175. doi: 10.1002/2013PA002523.
- Smart, C.W., Thomas, E., and Bracher, C.M. (2019). Holocene variations in North Atlantic export productivity as reflected in bathyal benthic foraminifera. *Mar. Micropaleontol.* 149, 1–18. doi: 10.1016/j.marmicro.2019.03.004.
- Thornalley, D.J., Oppo, D.W., Ortega, P., Robson, J.I., Brierley, C.M., Davis, R., et al. (2018). Anomalously weak Labrador Sea convection and Atlantic overturning during the past 150 years. *Nature* 556(7700), 227–230. doi: 10.1038/s41586-018-0007-4.